Int J Infrared Milli Waves (2007) 28:443–449
DOI 10.1007/s10762-007-9223-y

Parameters to Define the Electron Beam Trajectory of a Double-Tapered Disc-Loaded Wideband Gyro-TWT in Profiled Magnetic Field

Vishal Kesari · P. K. Jain · B. N. Basu

Received: 8 March 2007 / Accepted: 30 March 2007 /
Published online: 18 April 2007

Abstract In the method of tapering the cross section of the interaction structure for broadbanding a gyro-TWT, the different portions of the interaction length of the tapered-cross-section waveguide become effective for different frequency ranges if the magnetic field and beam parameters are profiled to maintain the condition of electron cyclotron resonance throughout the interaction length. In the present paper, the study of profiling the magnetic field and beam parameters in steps of the stepped analytical model of a double-tapered disc-loaded circular waveguide was made throughout the steps of the model. In the observed profile, the magnetic flux density in a typical step relative to its value in first-step decreases from first-step (gun-end) to end-step (collector-end) of the model considering the up-tapering schemes, in which structure parameters increase from gun-end to collector-end. Also, the transverse beam velocity in a typical step relative to its value in first-step decreases from gun-end to collector-end. However, the Larmor radius in a typical step relative to its value in first-step as well as the hollow-beam radius in a typical step relative to its value in first-step, both increase from gun-end to collector-end in the model considering the up-tapering schemes.

Keywords Disc-loaded waveguide · Magnetic field profile · Gyrotron · Wideband gyro-traveling-wave tube (gyro-TWT) · Millimeter-wave amplifier

1 Introduction

The developments of the gyrotrons, the gyro-klystrons and the gyro-TWTs have received the maximum attention in the development of gyro-devices [1–4]. The gyrotrons find application as high-power millimeter-wave sources, for instance, in plasma heating for controlled

V. Kesari (✉)
Department of Electronics and Communication Engineering, Birla Institute of Technology, Mesra, Ranchi 835 215, India
e-mail: vishal_kesari@rediffmail.com

P. K. Jain · B. N. Basu
Centre of Research in Microwave Tubes, Department of Electronics Engineering, Institute of Technology, Banaras Hindu University, Varanasi 221 005, India

thermonuclear reactor and in material processing. However, for applications in which coherent power combining is required, say, for phased-array radar, an amplifier like the gyro-TWT would be preferred to a source like the gyrotron [1–4]. Further, the use of an amplifier makes the data processing in radars rather simpler and better. Out of the gyro-klystron and the gyro-TWT, which have been successfully developed so far, the former that employs resonant interaction cavities, as in the conventional slow-wave klystron, has a lesser bandwidth than the latter that uses a non-resonant waveguide interaction structure [1–4]. Therefore, the gyro-klystron amplifiers, though they have potential applications in linear accelerators, are not preferred to the gyro-TWTs, which have a wider bandwidth potential, for application in high information density communication systems and high-resolution radars in the high-power, millimeter-wave frequency regime [3, 4].

However, the gyro-TWT has a limited bandwidth due to the dispersion of the waveguide interaction structure of the device, which is operated close to waveguide cutoff frequency [3]. There are two methods of broadbanding a gyro-TWT in vogue. In the first of these methods, the conventional waveguide interaction structure is loaded by a dielectric [5] or made to deviate from a simple smooth-wall geometry, such as the geometry obtained by corrugating the waveguide-wall, like helical waveguide [6], disc-loaded waveguide [7, 8] *etc.* and also the geometry obtained by combined dielectric and metal loading [9]. Thus, the dispersion characteristics of the waveguide are controlled for wideband coalescence between the beam-mode and waveguide-mode dispersion characteristics [5–9]. In this method, the structure cross-sectional dimensions are held uniform over the interaction length. In the second method of widening the device bandwidth, the waveguide cross-sectional dimensions of the structure are not held uniform and rather they are tapered, and, at the same time, the magnetic field and the beam parameters are synchronously profiled in order to maintain the condition of cyclotron resonance [3, 7, 8, 10–12]. In the latter method, although the bandwidth is increased due to different portions of the interaction length of the tapered-cross-section waveguide becoming effective for different frequency ranges, the gain of the device decreases due to the reduction in the effective interaction length of the device at each of such frequency ranges [7, 8]. Also, a method was suggested by Kesari *et al.* [7, 8] that accrues the advantages of both the methods of broadbanding a gyro-TWT, namely the method of tapering the waveguide cross section and the method of shaping the dispersion characteristics by disc loading a circular waveguide. Thus, they suggested a method of double tapering the structure cross section, more precisely by stepping the disc-hole and waveguide-wall radii [7, 8]. In this method, it is also necessary to profile the magnetic field and beam parameters in order to maintain the condition of electron cyclotron resonance in double-tapered disc-loaded circular waveguide. Consequently, Kesari *et al*. [7, 8] have convinced their method of double tapering the disc-loaded circular waveguide by comparing the gain-frequency responses of the gyro-TWTs taking non-tapered smooth-wall waveguide, non-tapered disc-loaded waveguide, tapered smooth-wall waveguide and tapered disc-loaded waveguide as the interaction structures. In their method taking smooth-wall waveguide as reference interaction structure, for the typical structure parameters, they have predicted 4% increase in device bandwidth and 7.5 dB (31%) increase in gain due to disc loading; 35% increase in device bandwidth at the cost of 7.2 dB (33%) device gain due to tapering of smooth-wall structure cross-section; and 52% increase in device bandwidth at a little cost of 4.6 dB (19%) device gain due to combining both the methods of broadbanding the gyro-TWT in double-tapered waveguide [7].

The objective of present paper is to profile the magnetic field and the beam parameters in order to address the synchronism condition in a double-tapered disc-loaded circular waveguide interaction structure (Fig. 1) for broadbanding a gyro-TWT. Thus, the tapering

schemes for a double-tapered circular waveguide has been presented and the relevant relations have been derived (Section 2). Also, the profile results have been plotted (Section 3) and the conclusion has been drawn (Section 4).

2 Profile of magnetic field and beam parameters

In a method of double tapering a disc-loaded circular waveguide (Fig. 1) for broadbanding a gyro-TWT, the following tapering or stepping schemes of the disc-hole radius and the waveguide-wall radius are assumed [7, 8]:

$$r_{D,p} = r_{D,1} + \frac{(p-1)}{(n_D-1)}\left(r_{D,n_D} - r_{D,1}\right) \tag{1}$$

$$r_{W,p} = r_{W,1} + \frac{(p-1)}{(n_D-1)}\left(r_{W,n_D} - r_{W,1}\right), \tag{2}$$

where the subscript $p(1 \le p \le n_D)$ with the waveguide-wall radius r_W and disc-hole radius r_D refers to the p^{th}-step of the parameter, thus $r_{W,p}$ and $r_{D,p}$ representing the waveguide-wall

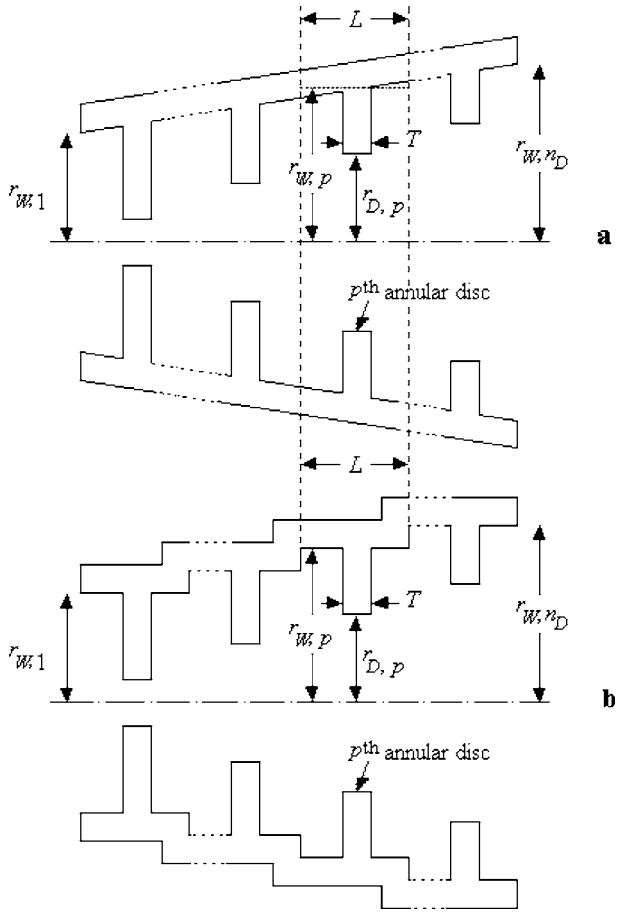

Fig. 1 Schematic of a double-tapered disc-loaded circular waveguide: (a) the actual structure and (b) its analytical model.

radius of the p^{th}-step and the disc-hole radius of the p^{th} disc, respectively, the latter positioned at the middle of the p^{th}-step length. Here, $p=1$ and $p=n_D$ would then refer to the start (gun-end) and the end (collector-end) steps, respectively (Fig. 1). Here, it should be noticed that the remaining structure parameters, namely the disc-to-disc distance L and the disc thickness T are kept uniform throughout the structure [7, 8].

Further, the cutoff angular frequency $\omega_{cut,p}$ of the p^{th}-step will change from step to step as p changes, as per the tapering schemes (1) and/ or (2). For the purpose of profiling the magnetic field, one has to maintain a constant ratio of the magnetic flux density $B_{0,p}$ in the structure with the corresponding grazing-point magnetic flux density $B_{g,p}$, given by $B_{g,p} = \left(m_{e0}\gamma\omega_{cut,p}/(|e|s)\right)\left(1 - v_{z,p}^2/c^2\right)^{1/2}$ [7, 10]:

$$\frac{B_{0,p}}{B_{g,p}} = \frac{|e|s\gamma_{z,p}B_{0,p}}{m_{e0}\gamma\omega_{cut,p}} = \frac{\omega_{c,p}s\gamma_{z,p}}{\gamma\omega_{cut,p}} = \text{constant}. \tag{3}$$

where $\omega_{c,p}\left(= eB_{0,p}/m_{e0}\right)$ is the nonrelativistic cyclotron angular frequency in the p^{th}-step of the stepped structure, e and m_{e0} are the electronic charge and rest mass, s is the beam harmonic number, $\nu_{z,p}$ and $\nu_{t,p}$ being the axial and transverse beam velocities in the p^{th}-step of the stepped analytical model of the structure, respectively. $\gamma\left(=\left[1-\left(\nu_{z,p}^2+\nu_{t,p}^2\right)/c^2\right]^{-1/2}\right)$ and $\gamma_{z,p}\left(=\left(1-\nu_{z,p}^2/c^2\right)^{-1/2}\right)$ are the relativistic mass factors with reference to the concerned electron velocities. γ may also be represented in terms of beam voltage V_0, by equating the relativistic kinetic energy with the potential energy of the electron beam, as $\gamma = 1 + |e|V_0/(m_{e0}c^2)$. It may be noted that γ does not vary from step-to-step [4]. In view of the constancy of γ, one may simplify (3), as follows:

$$\frac{\gamma_{z,p}B_{0,p}}{\omega_{cut,p}} = \text{constant}. \tag{4}$$

At the same time, it is implied that the beam parameters, namely, the transverse beam velocity $\nu_{t,p}$, the Larmor radius $r_{L,p}$, and the hollow-beam radius $r_{H,p}$, in the p^{th}-step, will vary from step to step as per the magnetic field profile [10, 12]. Thus, the combined magnetic field and beam parameters $\nu_{t,p}B_{0,p}^{-1/2}$, $r_{L,p}B_{0,p}^{1/2}$ and $r_{H,p}B_{0,p}^{1/2}$ individually maintain a constant value, throughout the length of the model $(1 \le p \le n_D)$, in order to obey the conservation of electron magnetic moment [12], the adiabatic beam-flow condition [13], and the conservation of magnetic flux [12], respectively. Thus, the beam parameters $\nu_{t,p,}$ $r_{L,p}$ and $r_{H,p}$ in the p^{th}-step may each be found in terms of the corresponding quantities of the first step, respectively, as:

$$\nu_{t,p}/\nu_{t,1} = \left(B_{0,p}/B_{0,1}\right)^{1/2}, \tag{5}$$

$$r_{L,p}/r_{L,1} = \left(B_{0,p}/B_{0,1}\right)^{-1/2} \tag{6}$$

and

$$r_{H,p}/r_{H,1} = \left(B_{0,p}/B_{0,1}\right)^{-1/2}. \tag{7}$$

Further, as discussed preceding (3), the magnetic flux density is tapered, but its value relative to the grazing-point value is kept the same [10]. One may obtain the magnetic field

taper parameter, which is the ratio of the magnetic flux density in the p^{th}-step to its value at the first step, from the solution of the following quadratic equation

$$\left(\frac{\omega_{cut,p}}{\omega_{cut,1}}\right)^{-2}\left(\frac{B_{0,p}}{B_{0.1}}\right)^{2}-\gamma_{z,p}^{2}\left(\frac{\nu_{t,p}}{c}\right)^{2}\left(\frac{B_{0,p}}{B_{0.1}}\right)-\left(\frac{\gamma_{z,1}}{\gamma}\right)^{2}=0,$$

which is obtained by combining (4) and (5), and making use of the definitions of γ and $\gamma_{z,p}$ given following (3). Thus, the magnetic flux density of the p^{th}-step relative to that of the first-step is obtained as

$$\frac{B_{0,p}}{B_{0,1}}=\frac{1}{2}\left[\left(\gamma_{z,p}\frac{\nu_{t,p}}{c}\right)^{2}+\left(\left(\gamma_{z,p}\frac{\nu_{t,p}}{c}\right)^{4}+4\left(\frac{\omega_{cut,p}}{\omega_{cut,1}}\right)^{-2}\left(\frac{\gamma_{z,1}}{\gamma}\right)^{2}\right)^{1/2}\right]\left(\frac{\omega_{cut,p}}{\omega_{cut,1}}\right)^{2}. \quad (8)$$

In the calculation of $B_{0,p}/B_{0,1}$ using (8), the angular cutoff frequencies in a particular step may be found from the eigenvalue obtained from the dispersion relation of the disc-loaded circular waveguide [7, 8] for the corresponding step dimensions; and the relativistic mass factor γ may be calculated in terms of beam voltage V_0 using the expression preceding to (4). Further, one may obtain $\gamma_{z,p}$ in terms of γ and beam pitch factor α_0, by equating the two expressions for $\nu_{z,p}$, one by substituting $\nu_{t,p}=\alpha_0\nu_{z,p}$ into definition of γ, and other by the definition of $\gamma_{z,p}$, i.e. $\nu_{z,p}=c\left(1-\gamma_{z,p}^{-2}\right)^{1/2}$. Once $\gamma_{z,p}$ is known, $\nu_{t,p}$ may be calculated by the relation $\nu_{t,p}=\alpha_0 c\left(1-\gamma_{z,p}^{-2}\right)^{1/2}$. Thus, the transverse beam velocity, the Larmor radius and the hollow beam radius, in the pth-step may be calculated, respectively, using (8) in each of (5), (6) and (7) in terms of the corresponding parameters in the first-step of stepped analytical model of a double-tapered disc-loaded circular waveguide.

3 Results and discussion

Reportedly [7], for the TE_{01} mode excitation, the parameter r_D, which has been found to control the gyro-TWT performances with respect to the gain, bandwidth and mid-band frequency to an appreciable extent for the device in a non-tapered disc-loaded circular waveguide, significantly influences these performances of the device in the tapered structure, too, as per scheme (1). Also, the parameter r_W, as per scheme (2), controls the device gain without much affecting the bandwidth and the mid-band frequency of the device. Thus, the tapering or stepping of the parameter r_D according to scheme (1) spreads the amplification band over a relatively wide frequency range, however, at the cost of the device gain obtainable in a non-tapered structure of a relatively larger value of r_D. This prompts to combine the tapering schemes (1) and (2), with a view to spreading the frequency range of amplification over a wideband and enhancing the device gain that would deteriorate at the band edges if the parameter r_D were tapered. Correspondingly, for the tapering schemes (1) and (2) combined, care should be taken to synchronously profile the magnetic flux density (Fig. 2), and accordingly also the relevant beam parameters, namely the transverse beam velocity according to (5), the Larmor radius $r_{L,p}$ according to (6), and the hollow-beam radius according to (7) (Fig. 3). Under the consideration of up-tapering scheme $\left(r_{w,n_D}>r_{W,1},\quad r_{D,n_D}>r_{D,1}\right)$, in which the parameters waveguide-wall radius and disc-hole radius increase from gun-end to collector-end $\left(r_{w,p}>r_{W,p-1},\quad r_{D,p}>r_{D,p-1}\right)$, while the magnetic flux density relative to its grazing point value in the p^{th}-step maintains constancy, the magnetic flux density in the p^{th}-step relative to its value in first-step continuously decreases from first-step (p=1: gun-end) to end-step ($p=n_D$: collector-end)

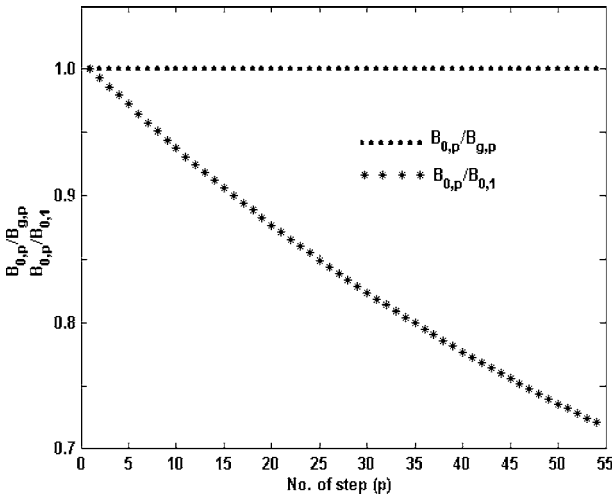

Fig. 2 Magnetic field profile with respect to the taper steps in a double-tapered disc-loaded circular waveguide typically at 40 GHz. The typical structure parameters are n_D=54, T=1.0 mm and L=3.0 mm; the typical waveguide excitation mode is TE_{01}; and the beam parameters are typically $r_{H,1}$=3.5 mm, $r_{L,1}/r_{W,1} = 0.1$, I_0=9.0 A, V_0= 100 kV, and α_0=0.5.

(Fig. 2). Similarly, considering up-tapering scheme, the transverse beam velocity in the p^{th}-step relative to its value in first-step continuously decreases from gun-end (p=1) to collector-end ($p=n_D$) (Fig. 3). However, the Larmor radius and the hollow-beam radius in the pth-step relative to their corresponding values in first-step, both continuously increase from gun-end (p=1) to collector-end ($p=n_D$) (Fig. 3) according to tapering schemes (1) and (2) combined in a double-tapered disc-loaded circular waveguide.

Although, in the present paper, up-tapering scheme $\left(r_{w,n_D} > r_{W,1}, \quad r_{D,n_D} > r_{D,1}\right)$, in which the parameters waveguide-wall radius and disc-hole radius increase from gun-end to collector-end $r_{w,p} > r_{W,p-1}, \quad r_{D,p} > r_{D,p-1}$, has been presented, the analysis is equally valid for the down-tapering scheme $\left(r_{w,n_D} < r_{W,1}, \quad r_{D,n_D} < r_{D,1}\right)$, in which the parameters decrease from gun-end to collector-end $\left(r_{w,p} < r_{W,p-1}, \quad r_{D,p} < r_{D,p-1}\right)$. Thus, for the structure in down-tapering scheme and for the constant ratio of magnetic flux density and its grazing point value in the p^{th}-step, the magnetic flux density in the p^{th}-step relative to its value in first-step will continuously increase from gun-end (p=1) to collector-end ($p=n_D$). Similarly, the transverse beam velocity in the pth-step relative to its value in first-step will continuously increase from gun-end (p=1) to collector-end ($p=n_D$). However, the Larmor

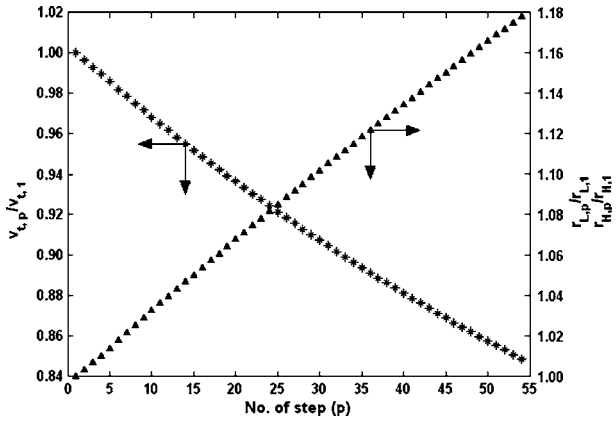

Fig. 3 Transverse beam velocity (asterisk marks), Larmor radius and hollow-beam radius (triangular marks) profiles with respect to the taper steps in a double-tapered disc-loaded circular waveguide typically at 40 GHz. The typical waveguide excitation mode, structure parameters and beam parameters are the same as in Fig. 2, and the magnetic field parameter is typically $B_{0,p}/B_{g,p} = 1.0 \quad (1 \le p \le n_D)$.

radius in the p^{th}-step relative to its value in first-step as well as the hollow-beam radius in the p^{th}-step relative to its value in first-step, both will continuously decrease from gun-end (p=1) to collector-end ($p=n_D$) under down-tapering schemes (1) and (2) combined in a double-tapered disc-loaded circular waveguide. A small signal analysis of the gyro-TWT has been used to address the beam-wave synchronism condition. However, the necessities are felt for the calculation of the interaction efficiency and sensitivity to the beam-velocity spread as well as the dynamical calculations to verify the bandwidth improvement, as presented by Chu *et al.* [12] for the tapered gyro-TWT and Nguyen *et al.* [11] for the two-stage tapered gyro-TWT, which have been kept outside the scope of the present paper.

4 Conclusion

In the present paper, profiles of the magnetic field and beam parameters in a waveguide having non-uniform cross-sectional dimensions, namely the double-tapered disc-loaded circular waveguide, have been developed considering the up-tapering scheme and the expected profiles for the down-tapering scheme have been presented. It is hoped that profiling the magnetic field and beam parameters in a double-tapered disc-loaded circular waveguide, developed in this paper, would maintain the condition of electron cyclotron resonance in each step and hence throughout the interaction length that would yield a broadband performance of a gyro-TWT.

References

1. R. J. Barker, J. H. Booske, N. C. Luhmann Jr., and G. S. Nusinovich, Ed., *Modern Microwave and Millimeter-Wave Power Electronics* (IEEE Press, New Jersey, 2004)
2. A. V. Gaponov-Grekhov and V. L. Granatstein, Ed., *Application of High Power Microwaves* (Artech House, Boston, 1994)
3. K. R. Chu, "The electron cyclotron maser." Rev. Mod. Phys. **76**, 489–540 (2004)
4. K. T. Nguyen, J. P. Calame, D. E. Pershing, B. G. Danly, M. Garven, B. Levush, and T. M. Antonsen Jr., "Design of a Ka-band gyro-TWT for radar applications." IEEE Trans. Electron. Dev. **48**, 108–115 (2001)
5. K. C. Leou, D. B. McDermott, and N. C. Luhmann Jr., "Dielectric loaded wideband gyro-TWT." IEEE Trans. Plasma Sci. **20**, 188–196 (1992)
6. G. G. Denisov, V. L. Bratman, A. W. Cross, W. He, A. D. R. Phelps, K. Ronald, S. V. Samsonov, and C. G. Whyte, "Gyrotron travelling wave amplifier with a helical interaction waveguide." Phys. Rev. Lett. **81**, 5680–5683 (1998)
7. V. Kesari, P. K. Jain, and B. N. Basu, "Exploration of a double-tapered disc-loaded circular waveguide for a wideband gyro-traveling-wave tube." IEEE Electron Dev. Lett. **27**, 194–197 (2006)
8. V. Kesari, P. K. Jain, and B. N. Basu, "Analysis of a tapered disc-loaded waveguide for a wideband Gyro-TWT." IEEE Trans. Plasma Sci., Special issue - High-Power Microwave Generation, **34**, 541–546 (2006)
9. V. Kesari, P. K. Jain, and B. N. Basu, "Modeling of axially periodic circular waveguide with combined dielectric and metal loading." J. Phy. D: Appl. Phy. **38**, 3523–3529, (2005)
10. M. Agrawal, G. Singh, P. K. Jain, and B. N. Basu, "Analysis of a tapered vane loaded broad-band gyro-TWT." IEEE Trans. Plasma Sci. **29**, 439–444 (2001)
11. K. T. Nguyen, G. S. Park, J. J. Choi, S. Y. Park, and R. K. Parker, "Effects of beam velocity spread on two-stage tapered gyro-TWT amplifier." IEEE Trans. Plasma Sci., **43**, 655–660 (1996)
12. K. R. Chu, Y. Y. Lau, L. R. Barnett, and V. L. Granatstein, "Theory of a wide-band distributed gyrotron traveling-wave amplifier." IEEE Trans. Electron. Dev. **28**, 866–871 (1981)
13. J. M. Baird and W. Lawson, "Magnetron injection gun (MIG) design for gyrotron applications." Int. J. Electronics **61**, 953–967 (1986)